Human Molecular Genetics, 2016, Vol. 25, No. 6 1129–1139

doi: 10.1093/hmg/ddv635
Advance Access Publication Date: 5 January 2016
Original Article

ORIGINAL ARTICLE

Nf1$^{+/-}$ monocytes/macrophages induce neointima formation via CCR2 activation

Waylan K. Bessler[1,2,3,†], Grace Kim[4,5,†], Farlyn Z. Hudson[4,5], Julie A. Mund[1,2], Raghuveer Mali[1,2,3], Keshav Menon[1,2], Reuben Kapur[1,2,3], D. Wade Clapp[1,2,3], David A. Ingram Jr[1,2,3] and Brian K. Stansfield[4,5,*]

[1]Herman B. Wells Center for Pediatric Research, [2]Department of Pediatrics and Neonatal-Perinatal Medicine and [3]Department of Biochemistry and Molecular Biology, Indiana University School of Medicine, Indianapolis, IN 46202, USA, [4]Department of Pediatrics and Neonatal-Perinatal Medicine and [5]Vascular Biology Center, Augusta University, Augusta, GA 30912, USA

*To whom correspondence should be addressed at: Department of Pediatrics, Augusta University, 1120 15th Street, BIW 6033, Augusta, GA 30912, USA. Tel: +1 7067212331; Fax: +1 7067217531; Email: bstansfield@gru.edu

Abstract

Persons with neurofibromatosis type 1 (NF1) have a predisposition for premature and severe arterial stenosis. Mutations in the *NF1* gene result in decreased expression of neurofibromin, a negative regulator of p21^{Ras}, and increases Ras signaling. Heterozygous *Nf1* (*Nf1*$^{+/-}$) mice develop a marked arterial stenosis characterized by proliferating smooth muscle cells (SMCs) and a predominance of infiltrating macrophages, which closely resembles arterial lesions from NF1 patients. Interestingly, lineage-restricted inactivation of a single *Nf1* allele in monocytes/macrophages is sufficient to recapitulate the phenotype observed in *Nf1*$^{+/-}$ mice and to mobilize proinflammatory CCR2+ monocytes into the peripheral blood. Therefore, we hypothesized that CCR2 receptor activation by its primary ligand monocyte chemotactic protein-1 (MCP-1) is critical for monocyte infiltration into the arterial wall and neointima formation in *Nf1*$^{+/-}$ mice. MCP-1 induces a dose-responsive increase in *Nf1*$^{+/-}$ macrophage migration and proliferation that corresponds with activation of multiple Ras kinases. In addition, *Nf1*$^{+/-}$ SMCs, which express CCR2, demonstrate an enhanced proliferative response to MCP-1 when compared with WT SMCs. To interrogate the role of CCR2 activation on *Nf1*$^{+/-}$ neointima formation, we induced neointima formation by carotid artery ligation in *Nf1*$^{+/-}$ and WT mice with genetic deletion of either *MCP1* or *CCR2*. Loss of MCP-1 or CCR2 expression effectively inhibited *Nf1*$^{+/-}$ neointima formation and reduced macrophage content in the arterial wall. Finally, administration of a CCR2 antagonist significantly reduced *Nf1*$^{+/-}$ neointima formation. These studies identify MCP-1 as a potent chemokine for *Nf1*$^{+/-}$ monocytes/macrophages and CCR2 as a viable therapeutic target for NF1 arterial stenosis.

Introduction

Neurofibromatosis type 1 (NF1) is an autosomal dominant disorder affecting 1 in 3000 persons and is the result of inactivating mutations in the *NF1* tumor suppressor gene. Neurofibromin, the protein product of *NF1*, functions as a GTPase activating protein for p21^{ras} (Ras) and accelerates the slow, intrinsic hydrolysis of active Ras-GTP to its inactive diphosphate conformation (1). Inherited mutations of *NF1* affect a single gene copy and result in disease with complete penetrance and a broad range of clinical features.

Cardiovascular disease represents a common, yet understudied, manifestation of NF1 that contributes to the early mortality observed in this patient population (2). NF1 vasculopathy

[†]These authors contributed equally to this work.

Received: October 26, 2015. **Revised:** December 7, 2015. **Accepted:** December 30, 2015

primarily affects the arterial network with a strong predilection for the renal artery and proximal branches of the carotid artery. The exact frequency of vasculopathy in NF1 patients is unknown; however, multiple case series and large patient cohorts suggest the prevalence of arterial disease approaches 10% (3–7). The insidious and progressive clinical presentation of these lesions in early adulthood likely places the true incidence much higher. In fact, histologic evidence of cardiovascular disease was identified in nearly 50% of young adults with NF1 in one case series (8), whereas a comprehensive review of 3253 death certificates revealed a diagnosis of vasculopathy was listed 7.2 times more frequently than expected among NF1 patients less than 30 years of age at the time of death (4).

Arterial lesions associated with NF1 are characterized by smooth muscle cell (SMC) hyperplasia, leukocyte infiltration and arterial remodeling leading to vasoocclusion and tissue ischemia (2,9–11). Previously, we developed a mouse model of NF1 arterial stenosis using *Nf1* heterozygous ($Nf1^{+/-}$) mice that completely recapitulates the human phenotype (12). Although neointima formation is the result of complex interactions between vascular wall cells and circulating leukocytes, we showed that loss of a single *Nf1* allele in bone marrow cells is both necessary and sufficient to induce arterial stenosis (13). These results were somewhat surprising, because neurofibromin-deficient SMC have increased proliferation and migration in response to multiple growth factors and $Nf1^{+/-}$ macrophages (13,14). Neurofibromin-deficient macrophages are the dominant hematopoietic cell within the neointima of $Nf1^{+/-}$ mice and likely secrete cytokines and chemokines that stimulate SMC proliferation and migration (13,15). Thus, it is plausible that loss of neurofibromin in bone marrow and circulating hematopoietic cells, particularly monocytes and macrophages, may predispose NF1 patients to develop exaggerated responses to acute and chronic inflammation or insult. Emerging evidence in NF1 patients is supportive of this hypothesis. Asymptomatic NF1 patients have increased circulating proinflammatory cytokines and monocytes ($CD14^+CD16^+$) in the peripheral blood compared with controls (13). Similar to NF1 patients, $Nf1^{+/-}$ mice have increased circulating $Ly6C^{hi}CCR2^+$ monocytes, which are the murine correlate of human proinflammatory monocytes (15,16). Murine $Ly6C^{hi}CCR2^+$ leukocytes are primitive bone-marrow-derived monocytes that are actively recruited to sites of inflammation and differentiate into macrophages and inflammatory dendritic cells (17,18). In support of our hypothesis that neurofibromin regulates inflammatory cascades in circulating leukocytes, we recently showed that loss of a single *Nf1* gene copy in myeloid cells was sufficient to mobilize $Ly6C^{hi}CCR2^+$ monocytes and induce arterial stenosis following carotid artery ligation (15). Interestingly, genetic deletion of both *Nf1* gene copies in myeloid cells alone resulted in a 4-fold increase in circulating $Ly6C^{hi}CCR2^+$ monocytes and nearly complete arterial occlusion following carotid ligation (15).

Based on these observations, we generated compound mutant mice to test the hypothesis that CCR2 activation is critical for $Nf1^{+/-}$ macrophage recruitment to sites of vascular injury and necessary for $Nf1^{+/-}$ neointima formation. Further, we sought to understand how CCR2 activation by its primary ligand, monocyte chemotactic protein-1 (MCP-1/CCL2), mediates neurofibromin-deficient macrophage function and SMC proliferation. Finally, we use our murine model system to test the efficacy of a potent and specific inhibitor of the CCR2 receptor as a potential therapeutic intervention in the treatment of NF1 arterial stenosis.

Results

MCP-1 is a potent chemokine for $Nf1^{+/-}$ macrophages and SMC

MCP-1 is a monomeric polypeptide anchored to the endothelial monolayer of blood vessels and secreted by SMC and circulating leukocytes (19,20). The chemotactic properties of MCP-1 are primarily mediated through its activation of the CCR2 receptor (19,21–23). Importantly, the expression of CCR2 in the cardiovascular system is restricted to endothelial cells (ECs), SMC and monocytes/macrophages and is not a mediator of granulocyte chemotaxis (24–26). Therefore, we derived $Nf1^{+/-}$ and WT macrophages from $Nf1^{+/-}$ and WT mice to assess their functional response to MCP-1 stimulation. At baseline, $Nf1^{+/-}$ macrophages demonstrate a 2-fold increase in migration, but do not exhibit enhanced proliferation. In response to MCP-1 incubation, $Nf1^{+/-}$ macrophages exhibited a dose-dependent increase in chemotaxis and proliferation when compared with WT macrophages (Fig. 1A and B). Although MCP-1 also increased WT macrophage migration and proliferation in a dose-dependent manner, MCP-1 stimulated a 2- to 3-fold increase in $Nf1^{+/-}$ macrophage migration and proliferation when compared with WT macrophages at the same concentration of MCP-1. Interestingly, analysis of culture media from growth-arrested $Nf1^{+/-}$ and WT macrophages revealed an increased concentration of MCP-1 in the media of cultured $Nf1^{+/-}$ macrophages when compared with WT macrophage media (Fig. 1C). Cell counts of growth-arrested macrophages did not differ between genotypes (data not shown). Next, we analyzed neurofibromin-regulated Ras kinase activity to determine which pathway may be preferentially activated in in $Nf1^{+/-}$ macrophages in response to MCP-1 (Fig. 1D). While phosphorylation of both Erk and Akt was demonstrated in $Nf1^{+/-}$ macrophages incubated with MCP-1, the increase in p-Erk/Erk ratio did not differ between $Nf1^{+/-}$ and WT macrophages incubated with MCP-1 and likely represents an increase in Erk activity that is independent of neurofibromin expression. Akt phosphorylation, on the other hand, was dramatically higher in $Nf1^{+/-}$ macrophages stimulated with MCP-1 when compared with WT macrophages stimulated with MCP-1. Thus, $Nf1^{+/-}$ macrophages exhibit an exaggerated response to MCP-1 stimulation that corresponds with preferential activation of the PI3-K–Akt pathway.

Infiltrating macrophages secrete growth factors and cytokines to induce SMC proliferation and inward remodeling, which are hallmarks of arterial stenosis. Although genetic deletion of *Nf1* in SMC is not required for $Nf1^{+/-}$ neointima formation, $Nf1^{+/-}$ SMCs demonstrate enhanced proliferation in response to multiple growth factors and co-incubation with $Nf1^{+/-}$ and WT macrophages (14,15,27). Based on the observation that $Nf1^{+/-}$ macrophages exhibit increased production of MCP-1 and that SMC express CCR2, we isolated SMC from WT, $Nf1^{+/-}$ and $Nf1^{+/-}$; $CCR2^{-/-}$ mice to assess their proliferative response to MCP-1. Similar to previous published reports, WT SMC showed a modest proliferative response to MCP-1 (28–31) (Fig. 2A). While $Nf1^{+/-}$ SMCs are more proliferative at baseline, $Nf1^{+/-}$ SMC exhibited a nearly 2-fold increase in proliferation in response to MCP-1 stimulation when compared with untreated $Nf1^{+/-}$ SMC. MCP-1 expression in cultured $Nf1^{+/-}$ SMC and secretion into growth media was similar to WT SMC (data not shown). Genetic deletion of CCR2 in $Nf1^{+/-}$ SMC completely abolished the proliferative response mediated by MCP-1 and demonstrates that MCP-1 is primarily activating CCR2 on $Nf1^{+/-}$ SMC (Fig. 2A). Examination of Ras-dependent kinase activity revealed a profound increase in Erk signaling in $Nf1^{+/-}$ SMC stimulated with MCP-1 when

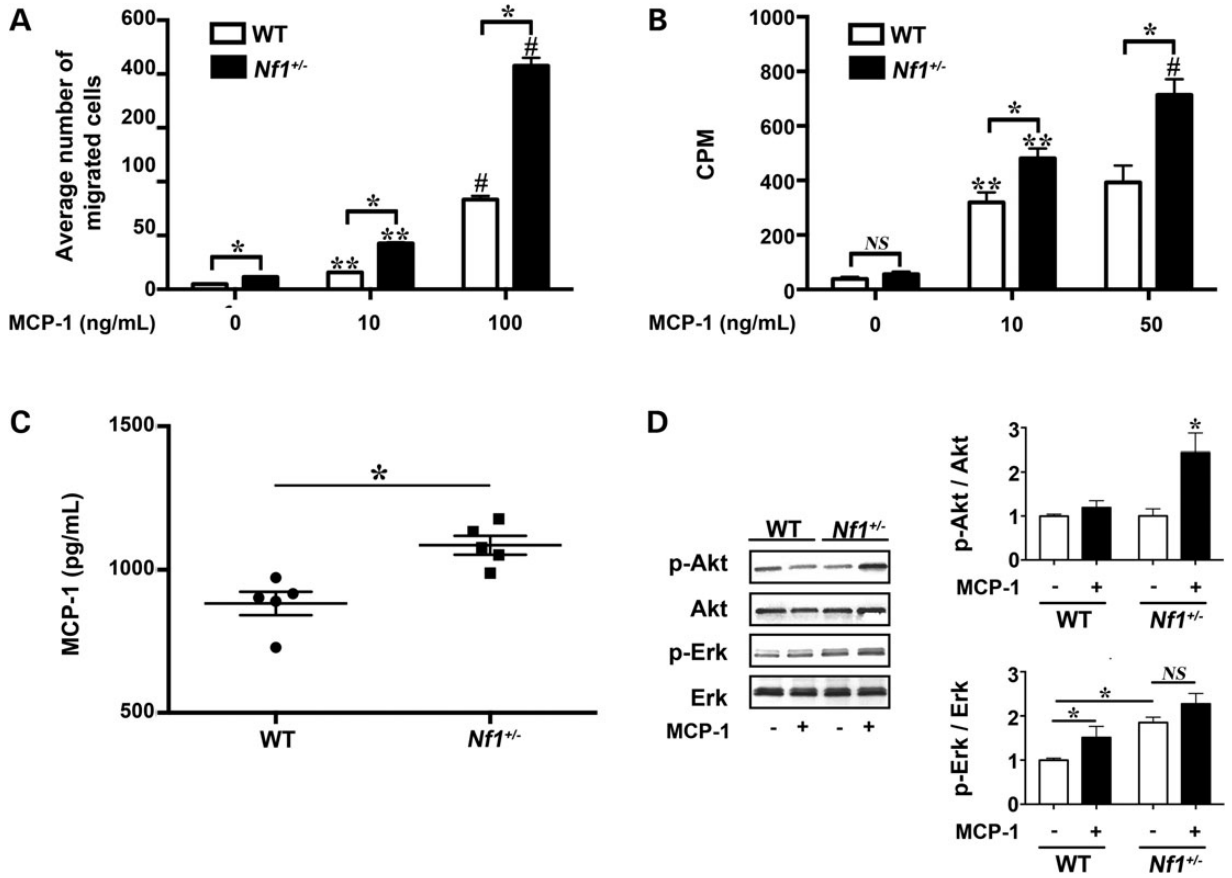

Figure 1. MCP-1 enhances $Nf1^{+/-}$ macrophage function. WT (white bars) and $Nf1^{+/-}$ (black bars) macrophage migration and proliferation, in response to MCP-1. (**A**) Data represent average number of migrated cells per HPF ± SEM, $n = 5$. *$P < 0.001$ for WT versus $Nf1^{+/-}$ macrophages at indicated concentration of MCP-1. **$P < 0.001$ for unstimulated WT and $Nf1^{+/-}$ macrophages versus MCP-1 (10 ng/ml) stimulated WT and $Nf1^{+/-}$ macrophages. #$P < 0.0001$ for MCP-1 (10 ng/ml) stimulated WT and $Nf1^{+/-}$ macrophages versus MCP-1 (100 ng/ml) stimulated WT and $Nf1^{+/-}$ macrophages. (**B**) Data represent thymidine incorporation reported as mean counts per minute (cpm) ± SEM, $n = 5$. *$P < 0.001$ for WT versus $Nf1^{+/-}$ macrophages at indicated concentration of MCP-1. **$P < 0.001$ for unstimulated WT and $Nf1^{+/-}$ macrophages versus MCP-1 (10 ng/ml) stimulated WT and $Nf1^{+/-}$ macrophages. #$P < 0.001$ for MCP-1 (10 ng/ml) stimulated $Nf1^{+/-}$ macrophages versus MCP-1 (50 ng/ml) stimulated $Nf1^{+/-}$ macrophages. (**C**) Data represent MCP-1 concentration reported as pg/ml ± SEM, $n = 5$. *$P < 0.01$ for WT versus $Nf1^{+/-}$ macrophage-conditioned media. (**D**) Representative western blots of Akt and Erk phosphorylation in WT and $Nf1^{+/-}$ macrophages treated with/without MCP-1 (10 ng/ml), $n = 4$. Quantitative densitometry ± SEM is reported as ratio of phosphorylated-Akt to total Akt or phosphorylated-Erk to total Erk density and corrected to unstimulated WT macrophages. *$P < 0.001$ for pAkt/Akt ratio in all conditions versus $Nf1^{+/-}$ macrophages stimulated with MCP-1. *$P < 0.01$ for pErk/Erk ratio for unstimulated WT macrophages versus MCP-1 stimulated WT macrophages and unstimulated $Nf1^{+/-}$ macrophages.

compared with unstimulated $Nf1^{+/-}$ SMC (Fig. 2B). MCP-1 did not alter Akt activity in $Nf1^{+/-}$ SMC (data not shown). Based on the substantial increase in Erk activity in response to MCP-1, we incubated $Nf1^{+/-}$ and WT SMC with MCP-1 (10 ng/ml) in the presence or absence of PD0325901, a potent inhibitor of Mek–Erk signaling. At low nanomolar concentrations of PD0325901, MCP-1 failed to evoke a proliferative response in *Nf1*+/– SMC (Fig. 2C). Not surprisingly, blockade of Erk signaling also reduced WT SMC proliferation and strengthens the argument that Erk activation is critical for MCP-1 elicited SMC proliferation. Collectively, these data suggest that $Nf1^{+/-}$ SMC exhibit enhanced proliferation in response to MCP-1 via Erk activation.

Genetic deletion of MCP-1 or CCR2 abrogates $Nf1^{+/-}$ neointima formation

Based on our observations that MCP-1 is a potent stimulus for $Nf1^{+/-}$ macrophage and SMC, we sought to interrogate the role of MCP-1/CCR2 signaling in the pathogenesis $Nf1^{+/-}$ arterial stenosis. $Nf1^{+/-}$ mice were intercrossed with $MCP1^{-/-}$ mice to generate compound mutant $Nf1^{+/-}$;$MCP1^{-/-}$ mice. WT, $MCP1^{-/-}$, $Nf1^{+/-}$ and $Nf1^{+/-}$; $MCP1^{-/-}$ mice underwent surgical ligation of the right common carotid artery to induce neointima formation. In response to arterial injury, WT mice developed a modest neointima, whereas $Nf1^{+/-}$ mice developed a robust neointimal layer after arterial injury (Fig. 3). Genetic deletion of MCP-1 completely inhibited neointima formation in $Nf1^{+/-}$ mice. Morphometric analysis of serial cross sections revealed a 70% reduction in neointima area (Fig. 3B) and a 55% reduction in intima/media (I/M) ratio (Fig. 3C). Corresponding with the reduced neointima in $Nf1^{+/-}$ mice lacking MCP-1 expression, Mac-3+ macrophage staining in the neointimas of $Nf1^{+/-}$; $MCP1^{-/-}$ mice were significantly reduced when compared with $Nf1^{+/-}$ neointimas (10.4 ± 3.0% versus 17.3 ± 3.4% of total cell number, $P = 0.1$; Fig. 3D).

Although MCP-1 primarily binds to CCR2, recent evidence suggests that MCP-1 has non-CCR2-mediated effects in SMC including binding of the CCR4 receptor (32,33). Therefore, we intercrossed $Nf1^{+/-}$ and $CCR2^{-/-}$ mice to examine the role of CCR2 activation on $Nf1^{+/-}$ neointima formation and macrophage infiltration into the vascular wall. The common carotid arteries of

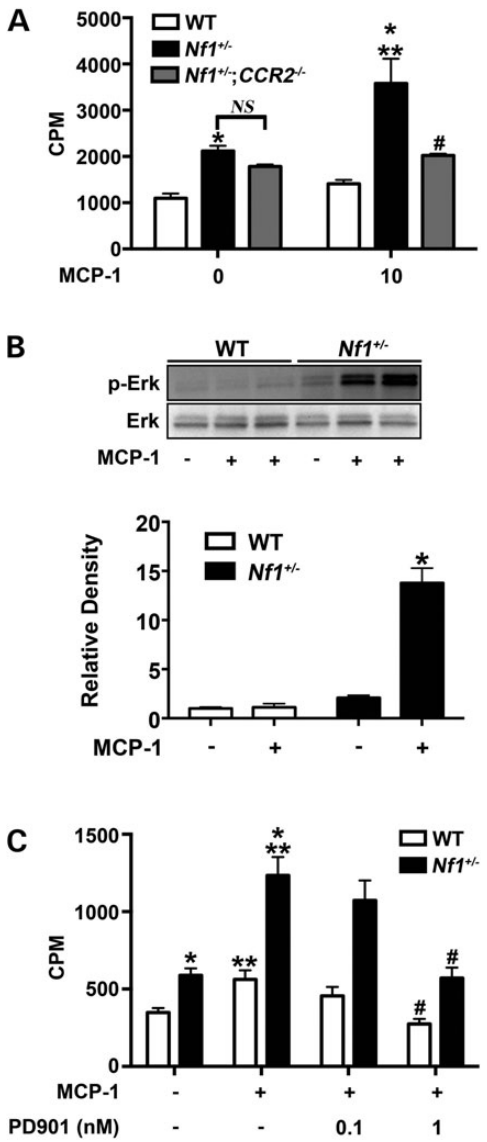

Figure 2. MCP-1 enhances $Nf1^{+/-}$ SMC proliferation via Erk activation. WT (white bars), $Nf1^{+/-}$ (black bars) and $Nf1^{+/-}$;$CCR2^{-/-}$ (gray bars) SMC proliferation in response to stimulation with MCP-1. (**A**) Data represent thymidine incorporation as mean cpm ± SEM, $n = 4$. *$P < 0.05$ for WT SMC versus $Nf1^{+/-}$ SMC at indicated concentrations of MCP-1. No statistical difference was observed between unstimulated $Nf1^{+/-}$ and $Nf1^{+/-}$;$CCR2^{-/-}$ SMC. **$P < 0.001$ for unstimulated $Nf1^{+/-}$ SMC versus MCP-1 stimulated $Nf1^{+/-}$ SMC. #$P < 0.001$ for MCP-1 stimulated $Nf1^{+/-}$ SMC versus MCP-1 stimulated $Nf1^{+/-}$;$CCR2^{-/-}$ SMC. (**B**) Representative western blot and quantitative densitometry of Erk phosphorylation in WT and $Nf1^{+/-}$ SMC treated with/without MCP-1 (10 ng/ml), $n = 3$. Quantitative densitometry ± SEM is reported as ratio for phosphorylated-Erk to total Erk density and corrected to unstimulated WT SMC. *$P < 0.0001$ for all conditions versus $Nf1^{+/-}$ SMC stimulated with MCP-1. (**C**) Data represent thymidine incorporation as mean cpm ± SEM, $n = 3$. *$P < 0.05$ for WT SMC versus $Nf1^{+/-}$ SMC at indicated concentrations of MCP-1. **$P < 0.01$ for unstimulated $Nf1^{+/-}$ and WT SMC versus MCP-1 stimulated $Nf1^{+/-}$ and WT SMC. #$P < 0.01$ for MCP-1 stimulated $Nf1^{+/-}$ and WT SMC versus MCP-1 stimulated $Nf1^{+/-}$ and WT SMC in the presence of PD0325901 at indicated concentration.

WT, $CCR2^{-/-}$, $Nf1^{+/-}$ and $Nf1^{+/-}$; $CCR2^{-/-}$ mice were ligated and analyzed for neointima formation after a 28-day recovery period. Similar to our previous experiment, $Nf1^{+/-}$ mice form a large neointima when compared with WT mice. Homozygous deletion of *CCR2* in $Nf1^{+/-}$ mice completely abrogated neointima formation and quantitative analysis of arterial cross sections demonstrated that arterial remodeling and neointima size were similar to WT arteries (Fig. 4A–C). Consistent with these observations, Mac-3+ macrophage infiltration into the neointima was reduced in $Nf1^{+/-}$;$CCR2^{-/-}$ mice when compared with $Nf1^{+/-}$ mice (12.2 ± 2.9% versus 21.53 ± 3.5% of total cell number, $P < 0.05$; Fig. 4D). Thus, MCP-1 and CCR2 expression are critical for neointima formation in $Nf1^{+/-}$ mice.

Pharmacologic inhibition of CCR2 inhibits $Nf1^{+/-}$ neointima formation

Pharmacologic inhibition of CCR2 could provide an attractive therapeutic target for NF1 patients with evidence of vasculopathy. Therefore, we utilized a specific CCR2 antagonist (INCB3284) for preclinical testing in our murine model system of NF1 arterial stenosis (34). $Nf1^{+/-}$ and WT mice were administered INCB3284 or vehicle via intraperitoneal injection immediately after arterial injury and once daily for 10 days as rescue therapy. This regimen was selected based on published pharmacokinetics for INCB3284 and specific targeting of macrophages during the early phase of arterial remodeling (34). In response to carotid artery ligation, vehicle-treated $Nf1^{+/-}$ mice developed significant intimal hyperplasia, whereas WT mice developed a more modest neointima, which was grossly and quantitatively similar to our previous observations (Fig. 5A–C). Daily administration of INCB 3284 as a rescue therapy significantly reduced neointima formation in $Nf1^{+/-}$ mice when compared with vehicle-treated $Nf1^{+/-}$ mice (Fig. 5B and C). While there was a trend toward reduction of neointima area and I/M ratio in WT mice treated with INCB 3284 when compared with WT mice receiving PBS treatment, statistical significance was not achieved ($P = 0.11$ and 0.5, respectively). Mac-3+ macrophage content was also reduced in $Nf1^{+/-}$ mice treated with INCB 3284 when compared with $Nf1^{+/-}$ mice receiving PBS treatment (16.3 ± 3.2% versus 24.12 ± 3.1% of total cell number, $P < 0.05$; Fig. 5D). Weight gain was similar between INCB 3284 and vehicle treatment groups, and no toxicities were observed on autopsy and inspection of visceral organs. These are the first data to suggest that a competitive CCR2 antagonist may be a viable therapeutic intervention for NF1 patients with evidence of cardiovascular disease.

Discussion

To date, therapeutic interventions for NF1 patients with cardiovascular disease have been limited, and tailored therapies directed at neurofibromin deficiency or its downstream targets are non-existent. Multiple extracellular signaling inputs converge on canonical Ras to maintain normal cell turnover, which limits the long-term use of Ras kinase inhibitors in patients with NF1 cardiovascular disease. Thus, a complete understanding of the pathogenesis of arterial disease in NF1 patients is imperative to inform novel therapeutic approaches leading to disease-specific clinical trials. Along this line of reasoning, emerging evidence suggests that NF1 patients experience chronic inflammation including increased cytokine production and frequency of circulating proinflammatory $CD14^{+}CD16^{+}$ monocytes in their peripheral blood (13). These findings are supported by our recent observation that $Nf1^{+/-}$ mice have increased circulating $Ly6C^{hi}$ monocytes, which closely resemble human proinflammatory intermediate monocytes (16). Increased cell surface expression of CCR2 is characteristic of $Ly6C^{hi}$ monocytes and enables these primitive myeloid cells to emigrate from the bone marrow and home to sites of inflammation where they differentiate into

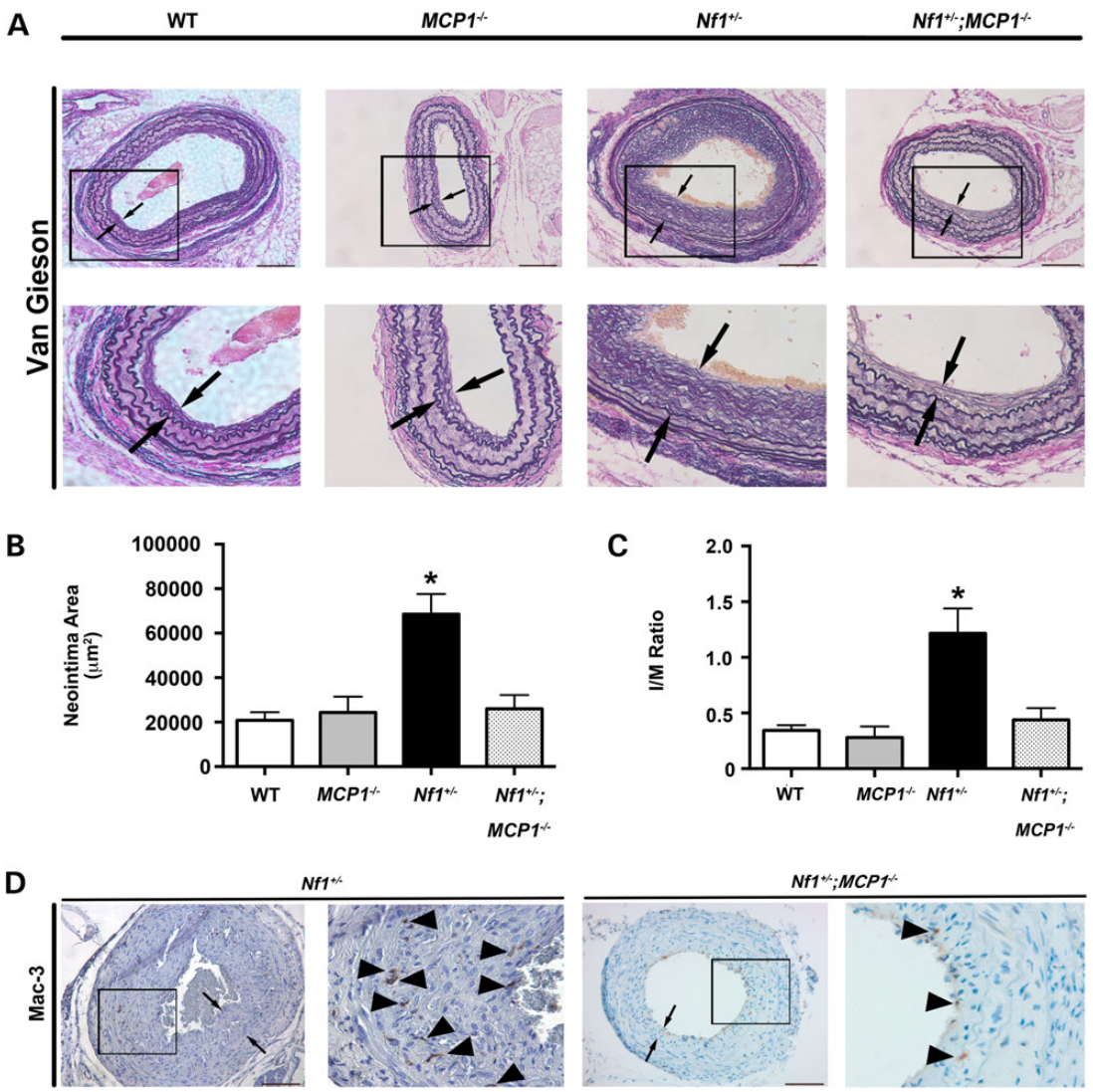

Figure 3. Genetic deletion of MCP-1 inhibits $Nf1^{+/-}$ neointima formation. Representative photomicrographs (**A**) and quantification of neointima area (**B** and **C**) of injured carotid arteries from WT, $MCP1^{-/-}$, $Nf1^{+/-}$ and $Nf1^{+/-}$;$MCP1^{-/-}$ mice. (A) Black arrows indicate neointima boundaries. Black boxes identify area of injured artery that is magnified below. Scale bars: 100 μm. (B and C) Quantification of neointima area (B) and I/M ratio (C) of injured carotid arteries from WT, $MCP1^{-/-}$, $Nf1^{+/-}$ and $Nf1^{+/-}$;$MCP1^{-/-}$ mice. Data represent mean neointima area or I/M ratio ± SEM, $n = 10–12$. *$P < 0.01$ for WT, $MCP1^{-/-}$ and $Nf1^{+/-}$;$MCP1^{-/-}$ mice versus $Nf1^{+/-}$ mice. (**D**) Representative photomicrographs of Mac-3 staining in injured carotid arteries from $Nf1^{+/-}$ and $Nf1^{+/-}$;$MCP1^{-/-}$ mice. Black arrows indicate neointima boundaries. Black box identifies area of injured artery that is magnified in the right column. Black arrowheads represent positive macrophage (anti-Mac3) staining. Scale bars: 100 μm.

macrophages and secrete growth factors, reactive oxygen species and cytokines (35). Neurofibromin appears to play a central role in their derivation and mobilization from the bone marrow. Similar to $Nf1^{+/-}$ mice, mice harboring a lineage-restricted deletion of a single *Nf1* gene copy in myeloid cells have increased Ly6-C^{hi}CCR2+ monocytes in the peripheral blood (15). Interestingly, genetic deletion of both *Nf1* gene copies resulted in a 4-fold increase in circulating Ly6C^{hi}CCR2+ monocyte frequency, which strongly suggests that neurofibromin directly regulates monocyte mobilization and inflammation via a cell autonomous and gene-dosage-dependent mechanism (15).

Not surprisingly, monocytes and macrophages appear to play a central role in the pathogenesis of NF1-related arterial stenosis. Experimental ligation of the common carotid artery in mice harboring a myeloid-specific deletion of *Nf1* results in a robust neointima that is identical to $Nf1^{+/-}$ mice and NF1 patients. Deletion of both *Nf1* alleles in myeloid cells resulted in a near-total occlusion of the carotid artery after injury. Thus, neointima formation in *Nf1*-mutant mice is directly regulated by neurofibromin expression in myeloid cells via a gene-dosage-dependent mechanism. Based on the observation that neointima formation and CCR2+, inflammatory monocyte frequency is directly regulated by myeloid cell-specific mutations in the *Nf1* gene, we utilized MCP-1 and CCR2 knockout mice to specifically interrogate the role of neurofibromin in regulating CCR2-dependent monocyte mobilization and homing during cardiovascular remodeling. Here we show that loss of MCP-1 or CCR2 expression prevents macrophage infiltration into the arterial wall and abolishes neointima formation in $Nf1^{+/-}$ mice. The recruitment of bone marrow monocytes appears to be strongly linked to the presence and activation of CCR2. CCR2-deficient mice have a dramatic reduction in mature monocyte frequency in the peripheral blood, whereas the bone marrow appears to be enriched with primitive and precursor myeloid cells indicating that CCR2 participates in

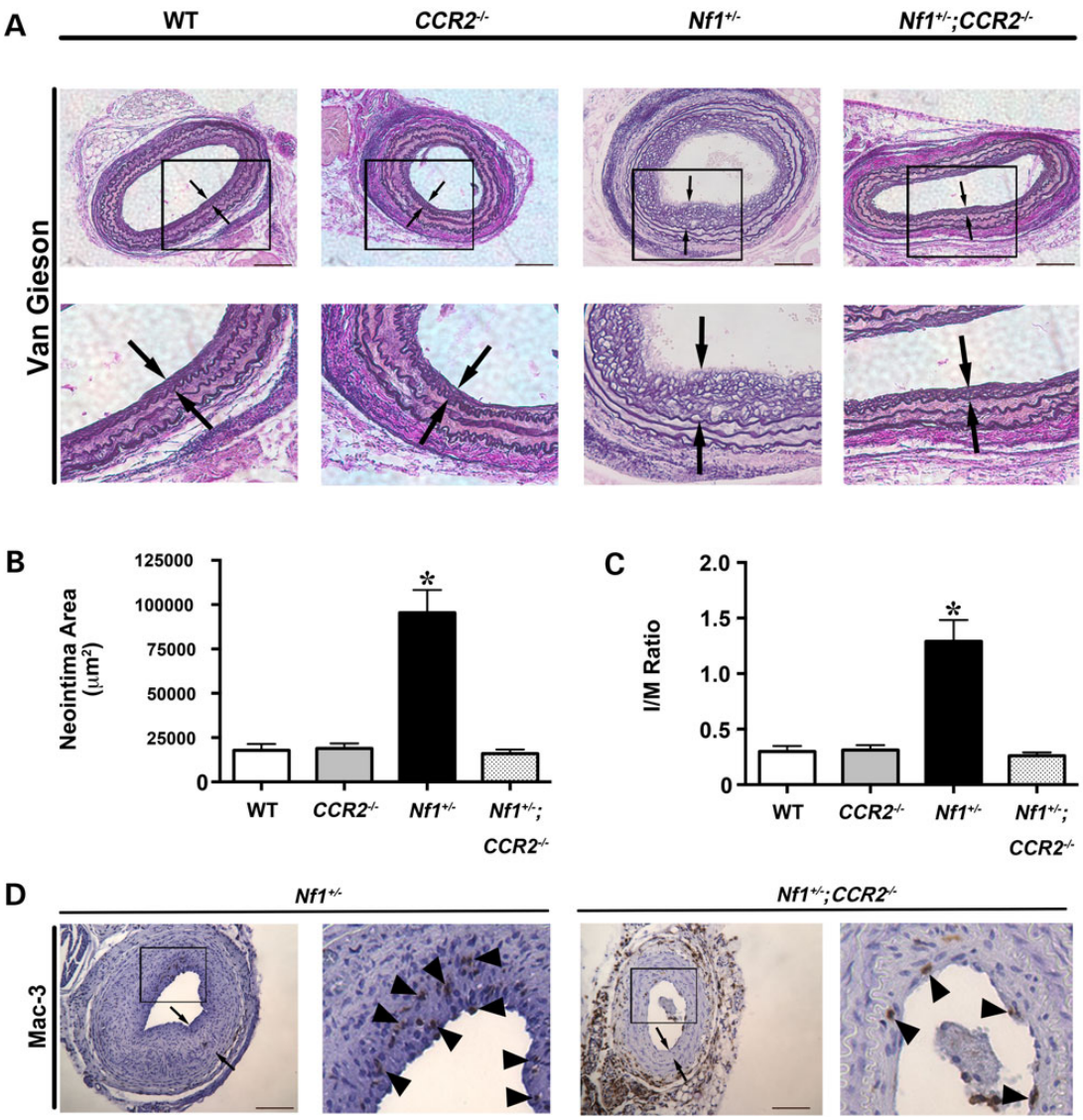

Figure 4. Genetic deletion of *CCR2* inhibits $Nf1^{+/-}$ neointima formation. Representative photomicrographs (**A**) and quantification of neointima area (**B** and **C**) of injured carotid arteries from WT, $CCR2^{-/-}$, $Nf1^{+/-}$ and $Nf1^{+/-}$;$CCR2^{-/-}$ mice. (A) Black arrows indicate neointima boundaries. Black boxes identify area of injured artery that is magnified below. Scale bars: 100 μm. (B and C) Quantification of neointima area (B) and I/M ratio (C) of injured carotid arteries from WT, $CCR2^{-/-}$, $Nf1^{+/-}$ and $Nf1^{+/-}$;$CCR2^{-/-}$ mice. Data represent mean neointima area or I/M ratio ± SEM, $n = 10–12$. *$P < 0.005$ for WT, $CCR2^{-/-}$ and $Nf1^{+/-}$;$CCR2^{-/-}$ mice versus $Nf1^{+/-}$ mice. (**D**) Representative photomicrographs of Mac-3 staining in injured carotid arteries from $Nf1^{+/-}$ and $Nf1^{+/-}$;$CCR2^{-/-}$ mice. Black arrows indicate neointima boundaries. Black box identifies area of injured artery that is magnified in the right column. Black arrowheads represent positive macrophage (anti-Mac3) staining. Scale bars: 100 μm.

the mobilization of monocytes from the bone marrow (25,36,37). Monocyte differentiation in $CCR2^{-/-}$ mice remains intact; however, mature monocytes fail to accumulate in the spleen and respond to inflammatory stimuli (36). Surprisingly, *CCR2* deletion failed to reduce neointima formation in our experimental model system. The demonstrated reduction in neointima formation in CCR2-deficient mice has largely been demonstrated in compound mutant mice (i.e. $CCR2^{-/-}$;$ApoE^{-/-}$) and may rely on a hyperlipidemic background to mediate its effects (38,39). Further, C57Bl/6 mice are highly resistant to arterial remodeling in multiple animal models, which is consistent with our experimental results and previous reports (12,13,15,27,40).

Although MCP-1 is the principal ligand for CCR2, other monocyte chemotactic proteins have affinity for CCR2 and have a role in monocyte function, SMC proliferation and arterial remodeling (25,41,42). Thus, complimentary studies in $Nf1^{+/-}$ mice lacking MCP-1 expression were critical to link the increased sensitivity of neurofibromin-deficient monocytes/macrophages to MCP-1 and the mobilization of CCR2+ proinflammatory monocytes in *Nf1*-mutant mice. The lack of neointima formation in $Nf1^{+/-}$;$MCP1^{-/-}$ mice mirrors our findings in *CCR2*-deficient $Nf1^{+/-}$ mice and provides strong genetic evidence that this signaling axis is necessary for $Nf1^{+/-}$ neointima formation. The underlying mechanisms of this interaction remain unclear; however, we show that MCP-1 preferentially activates Erk signaling in $Nf1^{+/-}$ SMC and multiple Ras-dependent kinases in $Nf1^{+/-}$ monocytes, including Akt. Interestingly, Erk and Akt, the primary downstream targets of Ras, activate several transcription factors including SP-1, c-Jun and AP-1, which control the expression of MCP-1 and other cytokines (43–46). In turn, expression of chemokines such as MCP-1 largely controls leukocyte and SMC function via RTK-mediated Ras activation. This may contribute to a positive feedback loop where

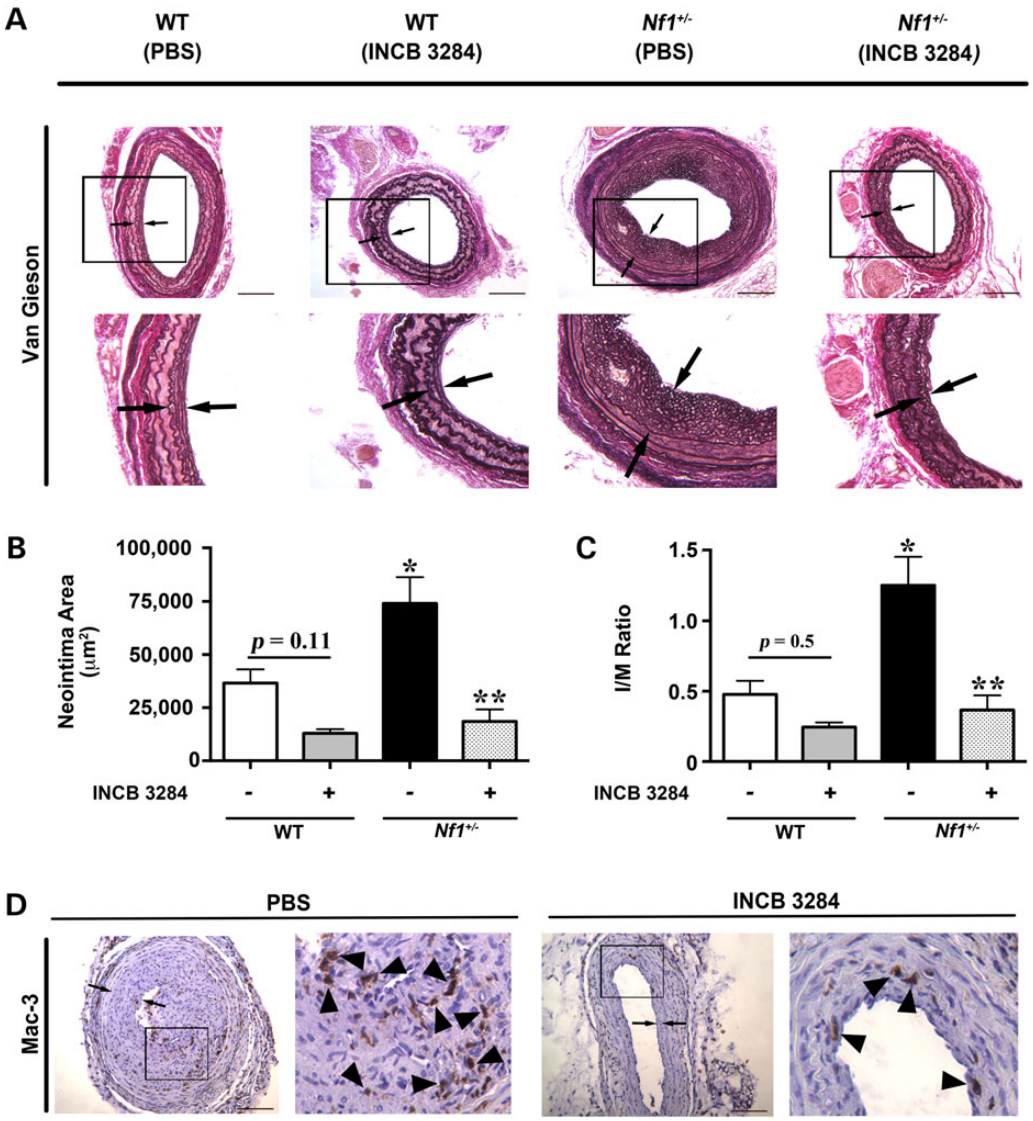

Figure 5. CCR2 antagonist reduces neointima formation in *Nf1*$^{+/-}$ mice. Representative photomicrographs (**A**) and quantification of neointima area (**B** and **C**) of injured carotid arteries from WT and *Nf1*$^{+/-}$ mice treated with INCB 3284 (15 mg/kg/day) or PBS. (A) Black arrows indicate neointima boundaries. Black boxes identify area of injured artery that is magnified below. Scale bars: 100 μm. (B and C) Quantification of neointima area (B) and I/M ratio (C) of injured carotid arteries from WT and *Nf1*$^{+/-}$ mice treated with INCB 3284 or PBS. Data represent mean neointima area or I/M ratio ± SEM, $n = 6–8$. *$P < 0.01$ for WT mice with PBS treatment versus *Nf1*$^{+/-}$ mice with PBS treatment. **$P < 0.001$ for *Nf1*$^{+/-}$ mice with PBS treatment versus *Nf1*$^{+/-}$ mice with INCB 3284 treatment. No statistically significant difference was observed between WT mice with PBS treatment and WT mice with INCB 3284 treatment. Experiments were performed in triplicate. (**D**) Representative photomicrographs of Mac-3 staining in injured carotid arteries from *Nf1*$^{+/-}$ mice with PBS treatment versus *Nf1*$^{+/-}$ mice with INCB 3284 treatment. Black arrows indicate neointima boundaries. Black box identifies area of injured artery that is magnified in the right column. Black arrowheads represent positive macrophage (anti-Mac3) staining. Scale bars: 100 μm.

cytokines can propagate their own production, which may be amplified in the setting of Ras deregulation (47–49). Our observation that neurofibromin-deficient macrophages have increased production and secretion of MCP-1, which may potentiate their own function, is congruent with this line of investigation. For example, mTOR signaling is proximally regulated by neurofibromin and loss of neurofibromin increases Akt activity in response to MCP-1 in murine monocytes. Recent studies in human and murine monocytes have revealed that MCP-1 production is directly regulated by mTOR activation and that inhibition of mTOR signaling results in decreased MCP-1 expression and secretion via an NF-κB-dependent mechanism. Interestingly genetic deletion of tuberous sclerosis complex 2 amplifies mTOR signaling and also increases MCP-1 expression, which suggests that this pathway directly regulates MCP-1 production. Therefore, it is plausible that decreased expression of neurofibromin may enhance downstream signaling networks that increase MCP-1 expression to provide a greater local concentration of MCP-1 to activate CCR2 on circulating monocytes/macrophages and vascular wall cells. While long-term use of an mTOR inhibitor for the prevention or treatment of NF1 vasculopathy is unlikely, interrogation of this pathway may provide substantial mechanistic insights into the regulation of monocyte-specific chemokines and their function in the setting of neurofibromin deficiency. Ongoing studies in our laboratory are focused on understanding how Ras signaling controls the transcription and/or activity of MCP-1.

Targeted therapies directed against either MCP-1 have yielded promising results in preclinical animal models, but have largely

proven to lack efficacy in human clinical trials (50–55). Bindarit, an indazolic derivative that binds to the promoter of the MCP-1 gene and limits MCP-1 expression, inhibits human and murine SMC proliferation and de-differentiation as well as neointima formation in several animal models (28,55,56). However, the use of a monoclonal antibody directed against MCP-1 in persons with rheumatoid arthritis did not improve clinical symptoms and demonstrated a dose-responsive increase in serum MCP-1 concentrations, which suggests that clearance of the antibody complex is limited (57). Antibodies directed against MCP-1 in the treatment of cardiovascular disease have not been proposed, though bindarit is presently under investigation for the treatment of diabetic nephropathy. MCP-1 may prove to be a difficult target for the treatment of cardiovascular disease because it is expressed and secreted by multiple cell types, including EC, SMC, leukocytes and perivascular adipocytes, and demonstrates affinity for other receptors including CCR4 (32,33). Further, MCP-1 secretion provides important feedback between perivascular cells (i.e. adipocytes) and remote tissues, including skeletal muscle and hepatocytes (58,59), which makes sequestering MCP-1 activity clinically difficult.

Local inhibition of CCR2, on the other hand, is an attractive therapeutic target for the treatment of NF1 vasculopathy because its expression and ligand-binding affinity is relatively limited. CCR2 antagonists have been studied in multiple clinical trials for the treatment of cardiovascular disease, autoimmunity, chronic inflammation, diabetes and malignancy (60–62). In particular, CCR2 antagonism may prove efficacious in the treatment of multiple manifestations of NF1, because acceleration of Ras activity in myeloid progenitor cells leads to dysfunctional differentiation and increased sensitivity to cytokines and growth factors (1,63–65). Our genetic and pharmacologic data support our hypothesis that MCP-1/CCR2 activation is highly regulated by neurofibromin and may represent a viable therapeutic target for NF1 patients with cardiovascular disease. Further studies directed at understanding how neurofibromin and/or Ras activation control the expression of MCP-1 and facilitate the mobilization of CCR2+ monocytes from the bone marrow are critical for future translational work and human studies of NF1 vasculopathy.

Materials and Methods

Animals

Protocols were approved by Laboratory Animal Services at Augusta University and Indiana University. *Nf1*$^{+/-}$ mice were obtained from Tyler Jacks (Massachusetts Institute of Technology, Cambridge, MA) and backcrossed 13 generations into the C57BL/6J strain. *MCP-1* (4434) and *CCR2* (4999) knockout mice were purchased from The Jackson Laboratory and maintained on C57BL/6 strain. *Nf1*$^{+/-}$ mice were intercrossed with *MCP1* and *CCR2* knockout mice to produce *Nf1*$^{+/-}$;*MCP1*$^{-/-}$ and *Nf1*$^{+/-}$;*CCR2*$^{-/-}$ mice. Male mice (12–15 weeks of age) were used for experiments to limit the confounding effects of circulating hormones.

Carotid artery ligation

Carotid artery injury was induced by ligation of the right common carotid artery as described (15). Briefly, mice were anesthetized by inhalation of an isoflurane (2%)/oxygen (98%) mixture. Under a dissecting scope, the right carotid artery was exposed through a midline neck incision and ligated proximal to the bifurcation using a 6–0 silk suture. The contralateral carotid artery was sham ligated as a control. Mice were administered 15 μg of buprenorphine (ip) following the procedure and recovered for 28 days. In some experiments, *Nf1*$^{+/-}$ and WT mice were administered 15 mg/kg INCB3284 (Caymen Chemical, IC_{50} 3.7 nM and $t_{½}$ 15 h) or vehicle via IP injection immediately after arterial injury and continued once daily for 10 days.

Morphometric analysis

Van Gieson-stained arterial cross sections 400, 800 and 1200 μm proximal to the ligation were analyzed for neointima formation using ImageJ (NIH, Bethesda, MD). Lumen area, area inside the internal elastic lamina (IEL), and area inside the external elastic lamina (EEL) were measured for each cross section. To account for potential thrombus formation, arteries containing significant thrombus (>50% lumen occlusion) at 400 μm proximal to the ligation were excluded from analysis. The number of excluded arteries was not different between experimental groups. Representative photomicrographs for each figure are taken from arterial cross sections between 600 and 1200 μm proximal to the bifurcation. Intima area was calculated by subtracting the lumen area from the IEL area, and the media area was calculated by subtracting the IEL area from the EEL area. I/M ratio was calculated as intima area divided by media area.

Histopathology and immunohistochemistry

For immunohistochemistry, serial sections were blocked for endogenous peroxidase activity with 3% hydrogen peroxide in methanol following antigen retrieval in Antigen Unmasking Solution (Vector Laboratories) at 95°C. Sections were blocked with Protein Block (Dako) for 1 h and were incubated with anti-Mac3 (1:50; BD Biosciences) primary antibodies. Sections were incubated with a biotinylated secondary antibody and visualized by 3,3′-diaminobenidine and counterstained with hematoxylin. Sections were examined, and images of sections were collected using a Zeiss Axioskop microscope (Carl Zeiss) with a 20× or 40× CP-ACHROMAT/0.12NA objective. Images were acquired using a SPOT RT color camera (Diagnostic Instruments). To quantify the number of macrophages within the neointima of each experimental group, Mac-3+ cells and SMCs were counted in three random 40× images by a blinded observer. To correct for a reduction in cell volume within the neointima, a ratio of Mac-3+ cells and SMC was calculated and analyzed for each mouse.

Isolation of bone-marrow-derived macrophages and characterization

Bone-marrow-derived macrophage isolation and characterization was performed as described (13). Proliferation was assessed by incorporation of radioactive thymidine in WT and *Nf1*$^{+/-}$ BM-derived macrophages. Briefly, WT and *Nf1*$^{+/-}$ macrophages (5×10^4 cells) were serum-starved for 12–18 h and placed in a 96-well plate in 200 μl starvation media in either the absence or presence of MCP-1 (10 ng/ml). Cells were cultured for 24 h and subsequently pulsed with 1.0 μCi (0.037 MBq) [^{3}H] thymidine for 6 h. Cells were harvested using a cell harvester and thymidine incorporation was determined as counts per minute (cpm).

For macrophage migration, the bottom of Transwell filters (8-μm pore filter; Costar) were coated with 20 μg/ml fibronectin CH296 peptide for 2 h at 37°C and rinsed twice with PBS containing 2% BSA. WT and *Nf1*$^{+/-}$ macrophages (2.5×10^5 cells) were placed in the upper chamber of the transwell and allowed to migrate toward the bottom of the transwell containing indicated

concentration of MCP-1. After 24 h, non-migrated cells in the upper chamber were removed with a cotton swab and migrated cells that attached to the bottom surface of the membrane were stained with 0.1% crystal violet dissolved in 0.1 M borate, pH 9.0 and 2% ethanol for 5 min at room temperature. The number of migrated cells was determined in five random fields with an inverted microscope using a 20 × objective lens. All experiments were performed in triplicate.

Smooth muscle cell isolation and proliferation

SMC isolation and proliferation assays were performed as described (14). SMCs were obtained by outgrowth from explants of WT, $Nf1^{+/-}$ and $Nf1^{+/-}$;$CCR2^{-/-}$ thoracic aortas. SMCs were cultured in DMEM supplemented with 10% fetal bovine serum and 100 U/ml penicillin/streptomycin in a 37°C, 5% CO_2-humidified incubator. For cell proliferation, SMC (5000 cells/cm^2) were placed in a 96-well plate and deprived of growth factors for 12–18 h. Quiescent SMC were stimulated with MCP-1 (10 ng/ml) for 24 h and pulse-labeled with 1 µCi/ml of [^{3}H] thymidine for 6 h. Beta emission was measured and reported as cpm. In some experiments, SMCs were incubated with indicated concentrations of PD0325901 (Erk inhibitor). All experiments were performed in triplicate.

Statistical analysis

All values are presented as mean or percent ± SEM. Cell proliferation and migration were analyzed by two-way ANOVA with Tukey's post hoc test for multiple comparisons. All experiments were performed in triplicate. MCP-1 concentration was analyzed by Student's *t*-test. Intima area and I/M ratio analysis was assessed by one-way ANOVA with Tukey's post hoc test for multiple comparisons. Murine experiments utilizing INCB 3284 were analyzed using two-way ANOVA with Tukey's post hoc test for multiple comparisons. Percent Mac-3+ cells was analyzed by Student's *t*-test. Analysis was performed using GraphPad Prism version 5.0d. $P < 0.05$ were considered significant.

Conflict of Interest statement. None declared.

Funding

This work is supported by the Department of Defense (NF140031, B.K.S.), the American Heart Association (15SDG2550005, B.K.S.), the Department of Pediatrics at Augusta University (B.K.S.) and the National Institutes of Health (P50 NS052606, D.A.I.).

References

1. Staser, K., Park, S.J., Rhodes, S.D., Zeng, Y., He, Y.Z., Shew, M. A., Gehlhausen, J.R., Cerabona, D., Menon, K., Chen, S. *et al.* (2013) Normal hematopoiesis and neurofibromin-deficient myeloproliferative disease require Erk. *J. Clin. Invest.*, **123**, 329–334.
2. Friedman, J.M., Arbiser, J., Epstein, J.A., Gutmann, D.H., Huot, S.J., Lin, A.E., McManus, B. and Korf, B.R. (2002) Cardiovascular disease in neurofibromatosis 1: report of the NF1 cardiovascular task force. *Genet. Med.*, **4**, 105–111.
3. Oderich, G.S., Sullivan, T.M., Bower, T.C., Gloviczki, P., Miller, D.V., Babovic-Vuksanovic, D., Macedo, T.A. and Stanson, A. (2007) Vascular abnormalities in patients with neurofibromatosis syndrome type I: clinical spectrum, management, and results. *J. Vasc. Surg.*, **46**, 475–484.
4. Rasmussen, S.A., Yang, Q. and Friedman, J.M. (2001) Mortality in neurofibromatosis 1: an analysis using U.S. death certificates. *Am. J. Hum. Genet.*, **68**, 1110–1118.
5. Lin, A.E., Birch, P.H., Korf, B.R., Tenconi, R., Niimura, M., Poyhonen, M., Armfield Uhas, K., Sigorini, M., Virdis, R., Romano, C. *et al.* (2000) Cardiovascular malformations and other cardiovascular abnormalities in neurofibromatosis 1. *Am. J. Med. Genet.*, **95**, 108–117.
6. D'Arco, F., D'Amico, A., Caranci, F., Di Paolo, N., Melis, D. and Brunetti, A. (2014) Cerebrovascular stenosis in neurofibromatosis type 1 and utility of magnetic resonance angiography: our experience and literature review. *Radiol. Med.*, **119**, 415–421.
7. Rea, D., Brandsema, J.F., Armstrong, D., Parkin, P.C., deVeber, G., MacGregor, D., Logan, W.J. and Askalan, R. (2009) Cerebral arteriopathy in children with neurofibromatosis type 1. *Pediatrics*, **124**, e476–e483.
8. Salyer, W.R. and Salyer, D.C. (1974) The vascular lesions of neurofibromatosis. *Angiology*, **25**, 510–519.
9. Kanter, R.J., Graham, M., Fairbrother, D. and Smith, S.V. (2006) Sudden cardiac death in young children with neurofibromatosis type 1. *J. Pediatr.*, **149**, 718–720.
10. Hamilton, S.J. and Friedman, J.M. (2000) Insights into the pathogenesis of neurofibromatosis 1 vasculopathy. *Clin. Genet.*, **58**, 341–344.
11. Lie, J.T. (1998) Vasculopathies of neurofibromatosis type 1 (von Recklinghausen Disease). *Cardiovasc. Pathol.*, **7**, 97–108.
12. Lasater, E.A., Bessler, W.K., Mead, L.E., Horn, W.E., Clapp, D. W., Conway, S.J., Ingram, D.A. and Li, F. (2008) Nf1+/– mice have increased neointima formation via hyperactivation of a Gleevec sensitive molecular pathway. *Hum. Mol. Genet.*, **17**, 2336–2344.
13. Lasater, E.A., Li, F., Bessler, W.K., Estes, M.L., Vemula, S., Hingtgen, C.M., Dinauer, M.C., Kapur, R., Conway, S.J. and Ingram, D.A. Jr. (2010) Genetic and cellular evidence of vascular inflammation in neurofibromin-deficient mice and humans. *J. Clin. Invest.*, **120**, 859–870.
14. Li, F., Munchhof, A.M., White, H.A., Mead, L.E., Krier, T.R., Fenoglio, A., Chen, S., Wu, X., Cai, S., Yang, F.C. *et al.* (2006) Neurofibromin is a novel regulator of RAS-induced signals in primary vascular smooth muscle cells. *Hum. Mol. Genet.*, **15**, 1921–1930.
15. Stansfield, B.K., Bessler, W.K., Mali, R., Mund, J.A., Downing, B., Li, F., Sarchet, K.N., DiStasi, M.R., Conway, S.J., Kapur, R. *et al.* (2013) Heterozygous inactivation of the Nf1 gene in myeloid cells enhances neointima formation via a rosuvastatin-sensitive cellular pathway. *Hum. Mol. Genet.*, **22**, 977–988.
16. Stansfield, B.K. and Ingram, D.A. (2015) Clinical significance of monocyte heterogeneity. *Clin. Transl. Med.*, **4**, 5.
17. Hilgendorf, I., Gerhardt, L.M., Tan, T.C., Winter, C., Holderried, T.A., Chousterman, B.G., Iwamoto, Y., Liao, R., Zirlik, A., Scherer-Crosbie, M. *et al.* (2014) Ly-6C high monocytes depend on Nr4a1 to balance both inflammatory and reparative phases in the infarcted myocardium. *Circ. Res.*, **114**, 1611–1622.
18. Robbins, C.S., Chudnovskiy, A., Rauch, P.J., Figueiredo, J.L., Iwamoto, Y., Gorbatov, R., Etzrodt, M., Weber, G.F., Ueno, T., van Rooijen, N. *et al.* (2012) Extramedullary hematopoiesis generates Ly-6C (high) monocytes that infiltrate atherosclerotic lesions. *Circulation*, **125**, 364–374.
19. Giunti, S., Pinach, S., Arnaldi, L., Viberti, G., Perin, P.C., Camussi, G. and Gruden, G. (2006) The MCP-1/CCR2 system has direct proinflammatory effects in human mesangial cells. *Kidney Int.*, **69**, 856–863.

20. Tieu, B.C., Lee, C., Sun, H., Lejeune, W., Recinos, A. 3rd, Ju, X., Spratt, H., Guo, D.C., Milewicz, D., Tilton, R.G. *et al.* (2009) An adventitial IL-6/MCP1 amplification loop accelerates macrophage-mediated vascular inflammation leading to aortic dissection in mice. *J. Clin. Invest.*, **119**, 3637–3651.
21. Sakai, N., Wada, T., Furuichi, K., Shimizu, K., Kokubo, S., Hara, A., Yamahana, J., Okumura, T., Matsushima, K., Yokoyama, H. *et al.* (2006) MCP-1/CCR2-dependent loop for fibrogenesis in human peripheral CD14-positive monocytes. *J. Leukoc. Biol.*, **79**, 555–563.
22. Lin, Y.M., Hsu, C.J., Liao, Y.Y., Chou, M.C. and Tang, C.H. (2012) The CCL2/CCR2 axis enhances vascular cell adhesion molecule-1 expression in human synovial fibroblasts. *PLoS ONE*, **7**, e49999.
23. Kalderen, C., Forsgren, M., Karlstrom, U., Stefansson, K., Svensson, R., Berglund, M.M., Palm, G., Selander, M., Sundbom, M., Nilsson, J. *et al.* (2012) A truncated analogue of CCL2 mediates anti-fibrotic effects on murine fibroblasts independently of CCR2. *Biochem. Pharmacol.*, **83**, 644–652.
24. Si, Y., Tsou, C.L., Croft, K. and Charo, I.F. (2010) CCR2 mediates hematopoietic stem and progenitor cell trafficking to sites of inflammation in mice. *J. Clin. Invest.*, **120**, 1192–1203.
25. Tsou, C.L., Peters, W., Si, Y., Slaymaker, S., Aslanian, A.M., Weisberg, S.P., Mack, M. and Charo, I.F. (2007) Critical roles for CCR2 and MCP-3 in monocyte mobilization from bone marrow and recruitment to inflammatory sites. *J. Clin. Invest.*, **117**, 902–909.
26. Hartl, D., Krauss-Etschmann, S., Koller, B., Hordijk, P.L., Kuijpers, T.W., Hoffmann, F., Hector, A., Eber, E., Marcos, V., Bittmann, I. *et al.* (2008) Infiltrated neutrophils acquire novel chemokine receptor expression and chemokine responsiveness in chronic inflammatory lung diseases. *J. Immunol.*, **181**, 8053–8067.
27. Stansfield, B.K., Bessler, W.K., Mali, R., Mund, J.A., Downing, B. D., Kapur, R. and Ingram, D.A. Jr. (2014) Ras-mek-erk signaling regulates nf1 heterozygous neointima formation. *Am. J. Pathol.*, **184**, 79–85.
28. Maddaluno, M., Grassia, G., Di Lauro, M.V., Parisi, A., Maione, F., Cicala, C., De Filippis, D., Iuvone, T., Guglielmotti, A., Maffia, P. *et al.* (2012) Bindarit inhibits human coronary artery smooth muscle cell proliferation, migration and phenotypic switching. *PLoS ONE*, **7**, e47464.
29. Porreca, E., Di Febbo, C., Reale, M., Castellani, M.L., Baccante, G., Barbacane, R., Conti, P., Cuccurullo, F. and Poggi, A. (1997) Monocyte chemotactic protein 1 (MCP-1) is a mitogen for cultured rat vascular smooth muscle cells. *J. Vasc. Res.*, **34**, 58–65.
30. Selzman, C.H., Miller, S.A., Zimmerman, M.A., Gamboni-Robertson, F., Harken, A.H. and Banerjee, A. (2002) Monocyte chemotactic protein-1 directly induces human vascular smooth muscle proliferation. *Am J Physiol. Heart Circ. Physiol.*, **283**, H1455–H1461.
31. Viedt, C., Vogel, J., Athanasiou, T., Shen, W., Orth, S.R., Kubler, W. and Kreuzer, J. (2002) Monocyte chemoattractant protein-1 induces proliferation and interleukin-6 production in human smooth muscle cells by differential activation of nuclear factor-kappaB and activator protein-1. *Arterioscler. Thromb. Vasc. Biol.*, **22**, 914–920.
32. Kim, M.S., Magno, C.L., Day, C.J. and Morrison, N.A. (2006) Induction of chemokines and chemokine receptors CCR2b and CCR4 in authentic human osteoclasts differentiated with RANKL and osteoclast like cells differentiated by MCP-1 and RANTES. *J. Cell. Biochem.*, **97**, 512–518.
33. Schecter, A.D., Berman, A.B., Yi, L., Ma, H., Daly, C.M., Soejima, K., Rollins, B.J., Charo, I.F. and Taubman, M.B. (2004) MCP-1-dependent signaling in CCR2(–/–) aortic smooth muscle cells. *J. Leukoc. Biol.*, **75**, 1079–1085.
34. Xue, C.B., Feng, H., Cao, G., Huang, T., Glenn, J., Anand, R., Meloni, D., Zhang, K., Kong, L., Wang, A. *et al.* (2011) Discovery of INCB3284, a potent, selective, and orally bioavailable hCCR2 antagonist. *ACS Med. Chem. Lett.*, **2**, 450–454.
35. Libby, P., Nahrendorf, M. and Swirski, F.K. (2013) Monocyte heterogeneity in cardiovascular disease. *Semin. Immunopathol.*, **35**, 553–562.
36. Serbina, N.V. and Pamer, E.G. (2006) Monocyte emigration from bone marrow during bacterial infection requires signals mediated by chemokine receptor CCR2. *Nat. Immunol.*, **7**, 311–317.
37. Ishibashi, M., Egashira, K., Zhao, Q., Hiasa, K., Ohtani, K., Ihara, Y., Charo, I.F., Kura, S., Tsuzuki, T., Takeshita, A. *et al.* (2004) Bone marrow-derived monocyte chemoattractant protein-1 receptor CCR2 is critical in angiotensin II-induced acceleration of atherosclerosis and aneurysm formation in hypercholesterolemic mice. *Arterioscler. Thromb. Vasc. Biol.*, **24**, e174–e178.
38. Liehn, E.A., Piccinini, A.M., Koenen, R.R., Soehnlein, O., Adage, T., Fatu, R., Curaj, A., Popescu, A., Zernecke, A., Kungl, A.J. *et al.* (2010) A new monocyte chemotactic protein-1/chemokine CC motif ligand-2 competitor limiting neointima formation and myocardial ischemia/reperfusion injury in mice. *J. Am. College Cardiol.*, **56**, 1847–1857.
39. Schober, A., Zernecke, A., Liehn, E.A., von Hundelshausen, P., Knarren, S., Kuziel, W.A. and Weber, C. (2004) Crucial role of the CCL2/CCR2 axis in neointimal hyperplasia after arterial injury in hyperlipidemic mice involves early monocyte recruitment and CCL2 presentation on platelets. *Circ. Res.*, **95**, 1125–1133.
40. Kuhel, D.G., Zhu, B., Witte, D.P. and Hui, D.Y. (2002) Distinction in genetic determinants for injury-induced neointimal hyperplasia and diet-induced atherosclerosis in inbred mice. *Arterioscler. Thromb. Vasc. Biol.*, **22**, 955–960.
41. Gong, X., Gong, W., Kuhns, D.B., Ben-Baruch, A., Howard, O.M. and Wang, J.M. (1997) Monocyte chemotactic protein-2 (MCP-2) uses CCR1 and CCR2B as its functional receptors. *J. Biol. Chem.*, **272**, 11682–11685.
42. Maddaluno, M., Di Lauro, M., Di Pascale, A., Santamaria, R., Guglielmotti, A., Grassia, G. and Ialenti, A. (2011) Monocyte chemotactic protein-3 induces human coronary smooth muscle cell proliferation. *Atherosclerosis*, **217**, 113–119.
43. Li, X. and Tai, H.H. (2013) Activation of thromboxane A2 receptor (TP) increases the expression of monocyte chemoattractant protein -1 (MCP-1)/chemokine (C-C motif) ligand 2 (CCL2) and recruits macrophages to promote invasion of lung cancer cells. *PLoS ONE*, **8**, e54073.
44. Lim, J.H., Um, H.J., Park, J.W., Lee, I.K. and Kwon, T.K. (2009) Interleukin-1beta promotes the expression of monocyte chemoattractant protein-1 in human aorta smooth muscle cells via multiple signaling pathways. *Exp. Mol. Med.*, **41**, 757–764.
45. Shimizu, H., Bolati, D., Higashiyama, Y., Nishijima, F., Shimizu, K. and Niwa, T. (2012) Indoxyl sulfate upregulates renal expression of MCP-1 via production of ROS and activation of NF-kappaB, p53, ERK, and JNK in proximal tubular cells. *Life Sci.*, **90**, 525–530.
46. Shang, F., Wang, J., Liu, X., Li, J., Zheng, Q., Xue, Y. and Zhao, L. (2012) Involvement of reactive oxygen species and JNK in increased expression of MCP-1 and infiltration of inflammatory cells in pressure-overloaded rat hearts. *Mol. Med. Rep.*, **5**, 1491–1496.

47. Jimenez-Sainz, M.C., Fast, B., Mayor, F. Jr and Aragay, A.M. (2003) Signaling pathways for monocyte chemoattractant protein 1-mediated extracellular signal-regulated kinase activation. *Mol. Pharmacol.*, **64**, 773–782.
48. Patial, S., Saini, Y., Parvataneni, S., Appledorn, D.M., Dorn, G. W. 2nd, Lapres, J.J., Amalfitano, A., Senagore, P. and Parameswaran, N. (2011) Myeloid-specific GPCR kinase-2 negatively regulates NF-kappaB1p105-ERK pathway and limits endotoxemic shock in mice. *J. Cell. Physiol.*, **226**, 627–637.
49. Yang, C.Q., Li, W., Li, S.Q., Li, J., Li, Y.W., Kong, S.X., Liu, R.M., Wang, S.M. and Lv, W.M. (2014) MCP-1 stimulates MMP-9 expression via ERK 1/2 and p38 MAPK signaling pathways in human aortic smooth muscle cells. *Cell. Physiol. Biochem.*, **34**, 266–276.
50. Arefieva, T.I., Krasnikova, T.L., Potekhina, A.V., Ruleva, N.U., Nikitin, P.I., Ksenevich, T.I., Gorshkov, B.G., Sidorova, M.V., Bespalova Zh, D., Kukhtina, N.B. *et al.* (2011) Synthetic peptide fragment (65–76) of monocyte chemotactic protein-1 (MCP-1) inhibits MCP-1 binding to heparin and possesses anti-inflammatory activity in stable angina patients after coronary stenting. *Inflamm. Res.*, **60**, 955–964.
51. Egashira, K., Nakano, K., Ohtani, K., Funakoshi, K., Zhao, G., Ihara, Y., Koga, J., Kimura, S., Tominaga, R. and Sunagawa, K. (2007) Local delivery of anti-monocyte chemoattractant protein-1 by gene-eluting stents attenuates in-stent stenosis in rabbits and monkeys. *Arterioscler. Thromb. Vasc. Biol.*, **27**, 2563–2568.
52. Nakano, K., Egashira, K., Ohtani, K., Zhao, G., Funakoshi, K., Ihara, Y. and Sunagawa, K. (2007) Catheter-based adenovirus-mediated anti-monocyte chemoattractant gene therapy attenuates in-stent neointima formation in cynomolgus monkeys. *Atherosclerosis*, **194**, 309–316.
53. Ohtani, K., Usui, M., Nakano, K., Kohjimoto, Y., Kitajima, S., Hirouchi, Y., Li, X.H., Kitamoto, S., Takeshita, A. and Egashira, K. (2004) Antimonocyte chemoattractant protein-1 gene therapy reduces experimental in-stent restenosis in hypercholesterolemic rabbits and monkeys. *Gene Ther.*, **11**, 1273–1282.
54. Zhao, Q. (2010) Dual targeting of CCR2 and CCR5: therapeutic potential for immunologic and cardiovascular diseases. *J. Leukoc. Biol.*, **88**, 41–55.
55. Ialenti, A., Grassia, G., Gordon, P., Maddaluno, M., Di Lauro, M. V., Baker, A.H., Guglielmotti, A., Colombo, A., Biondi, G., Kennedy, S. *et al.* (2011) Inhibition of in-stent stenosis by oral administration of bindarit in porcine coronary arteries. *Arterioscler. Thromb. Vasc. Biol.*, **31**, 2448–2454.
56. Grassia, G., Maddaluno, M., Guglielmotti, A., Mangano, G., Biondi, G., Maffia, P. and Ialenti, A. (2009) The anti-inflammatory agent bindarit inhibits neointima formation in both rats and hyperlipidaemic mice. *Cardiovasc. Res.*, **84**, 485–493.
57. Haringman, J.J., Gerlag, D.M., Smeets, T.J., Baeten, D., van den Bosch, F., Bresnihan, B., Breedveld, F.C., Dinant, H.J., Legay, F., Gram, H. *et al.* (2006) A randomized controlled trial with an anti-CCL2 (anti-monocyte chemotactic protein 1) monoclonal antibody in patients with rheumatoid arthritis. *Arthritis Rheum.*, **54**, 2387–2392.
58. Westerbacka, J., Corner, A., Kolak, M., Makkonen, J., Turpeinen, U., Hamsten, A., Fisher, R.M. and Yki-Jarvinen, H. (2008) Insulin regulation of MCP-1 in human adipose tissue of obese and lean women. *Am. J. Physiol. Endocrinol. Metab.*, **294**, E841–E845.
59. Younce, C. and Kolattukudy, P. (2012) MCP-1 induced protein promotes adipogenesis via oxidative stress, endoplasmic reticulum stress and autophagy. *Cell. Physiol. Biochem.*, **30**, 307–320.
60. Lin, K.L., Sweeney, S., Kang, B.D., Ramsburg, E. and Gunn, M. D. (2011) CCR2-antagonist prophylaxis reduces pulmonary immune pathology and markedly improves survival during influenza infection. *J. Immunol.*, **186**, 508–515.
61. Mildner, A., Mack, M., Schmidt, H., Bruck, W., Djukic, M., Zabel, M.D., Hille, A., Priller, J. and Prinz, M. (2009) CCR2+Ly-6Chi monocytes are crucial for the effector phase of autoimmunity in the central nervous system. *Brain*, **132**, 2487–2500.
62. Sullivan, T.J., Miao, Z., Zhao, B.N., Ertl, L.S., Wang, Y., Krasinski, A., Walters, M.J., Powers, J.P., Dairaghi, D.J., Baumgart, T. *et al.* (2013) Experimental evidence for the use of CCR2 antagonists in the treatment of type 2 diabetes. *Metabolism: Clin. Exp.*, **62**, 1623–1632.
63. Gritsman, K., Yuzugullu, H., Von, T., Yan, H., Clayton, L., Fritsch, C., Maira, S.M., Hollingworth, G., Choi, C., Khandan, T. *et al.* (2014) Hematopoiesis and RAS-driven myeloid leukemia differentially require PI3K isoform p110alpha. *J. Clin. Invest.*, **124**, 1794–1809.
64. Zeng, Y., Broxmeyer, H.E., Staser, K., Chitteti, B.R., Park, S.J., Hahn, S., Cooper, S., Sun, Z., Jiang, L., Yang, X. *et al.* (2015) Pak2 regulates hematopoietic progenitor cell proliferation, survival and differentiation. *Stem Cells*, **33**, 1630–1641.
65. Bollag, G., Clapp, D.W., Shih, S., Adler, F., Zhang, Y.Y., Thompson, P., Lange, B.J., Freedman, M.H., McCormick, F., Jacks, T. *et al.* (1996) Loss of NF1 results in activation of the Ras signaling pathway and leads to aberrant growth in haematopoietic cells. *Nat. Genet.*, **12**, 144–148.